Breast Cancer Associated Metastasis is Significantly Increased in a Model of Autoimmune Arthritis

Lopamudra Das Roy[1,2], Latha B. Pathangey[1], Teresa L. Tinder[1], and Pinku Mukherjee[1,2]*
[1]Department of Immunology, Mayo Clinic School of Medicine, Scottsdale, Arizona-85259
[2]Department of Biology, University of North Carolina at Charlotte, Charlotte, NC-28223

*Corresponding Author
Associate Professor,
Department of Immunology,
Mayo Clinic School of Medicine
Scottsdale, AZ-85259
mukherjee.pinku@mayo.edu
Current Address:
Irwin Belk Scholar for Cancer Research,
Associate Professor,
Department of Biology,
University of North Carolina at Charlotte,
Charlotte-NC-28223
pmukherj@uncc.edu
phone: 704-687-5459
fax: 704-687-3128

Supported by BCO63396 Concept Award (DOD Breast Cancer Research Program)

ABSTRACT

Chronic inflammation is known to play a role in cancer initiation, promotion, and metastasis. However, the mechanism by which inflammation promotes metastasis is still unclear. We evaluated if chronic inflammation induced by autoimmune arthritis may contribute to increased breast cancer-associated metastasis. We report a three-fold increase in lung metastasis and a significant increase in the incidence of bone metastasis in the pro-arthritic mice compared to control mice. The metastatic breast tumors in turn augment the severity of arthritis resulting in a vicious cycle that increases both bone destruction and metastasis. Enhanced neutrophilic and granulocytic infiltration in lungs and bone of the pro-arthritic mice and subsequent increase in circulating levels of proinflammatory cytokines, such as IL-17, IL-6, VEGF, and TNF-α were the underlying factors contributing to the increased metastasis. The data clearly has important clinical implications for patients diagnosed with metastatic breast cancer.

INTRODUCTION

Metastasis is regulated not only by intrinsic genetic changes in malignant cells, but also by the microenvironment. Several studies have demonstrated that sites of chronic inflammation are often associated with the establishment and growth of various malignancies [1]. A common inflammatory condition in humans is autoimmune arthritis (AA) that causes inflammation and deformity of the joints. Other systemic effects associated with AA include increased cellular infiltration and inflammation of the lungs and blood vessels (vasculitis), and weakening of the bones (osteoporosis). Although AA and cancer are different diseases, some of the underlying processes that contribute to the disorders of the joints and connective tissue that characterize AA also affect cancer progression and metastasis. In addition, the immune system appears to play an overseer's role in both diseases reviewed by Ziegler *et al* [2]**.** The most striking link between the two diseases came from a long-term community-based prospective study of the influence of inflammatory polyarthritis (IP) in cancer incidence and survival [3]. The authors reported that inflammatory arthritis increases the risk of dying from cancer (at least double the risk of general population). Several studies have also reported statistically significant risk ratios between AA and various malignancies including breast, lung, hematopoietic, non-melanotic skin, kidney, and colon **[4-6].**

Despite this knowledge available for a decade, there has been minimal research linking arthritis with metastatic breast cancer. It has never been questioned if a site of chronic inflammation linked to AA creates a milieu that attracts tumor cells to home and grow in the inflamed site. The lungs and bones are frequent sites of breast cancer metastasis [7].

The preference of breast cancer cells to grow in the bone and lung is underscored by the fact that 65-75% of patients with advanced disease develop bone or lung metastases [8]. Yet, it is not known why and how breast cancer cells prefer to colonize these organs. There are no methods to predict the risk of breast cancer-associated metastasis and current treatments have notable limitations. We hypothesize that chronic inflammatory milieu and osteoclastic bone resorption caused by AA and the lung inflammation associated with it may influence the recruitment, retention, and proliferation of tumor cells in the bone and lungs.

In this study, we determined if chronic inflammation in the bones and lungs induced by AA contribute to increased breast cancer-associated bone and lung metastasis. We have used a recently established animal model of spontaneous autoimmune arthritis known as the SKG mice. These mice are on the Balb/c background and carry a mutation of the gene encoding a SH2 domain of ZAP-70, a key signal transduction molecule in T cells and spontaneously develop T cell-mediated chronic AA [9]. The mutation impairs positive and negative selection of T cells in the thymus, leading to thymic production of arthritogenic autoimmune $CD4^+$ T cells. The mice succumb to symmetrical joint swelling beginning in the small joints of the digits and progressing to larger joints, accompanied by severe synovitis with formation of pannus invading and eroding adjacent cartilage and subchondral bone. Genetic deficiency of IL-6, IL-1, or TNF-α inhibit development of AA in SKG mice [10], similar to the effects of anticytokine therapy in human arthritis [11]. These clinical and immunopathological characteristics of AA in these mice make the strain a suitable model for testing our hypothesis. When these arthritic mice were induced to

develop metastatic mammary gland tumors, a significant increase in lung and bone metastasis were observed compared to the non-arthritic mice. Furthermore, the severity of arthritis was amplified by factors-associated with the metastatic compared to the non-metastatic tumor cells. We identified the key pro-inflammatory factors that contribute to the increased incidence of secondary metastasis and to the severity of the bone disease. A novel link between AA-induced inflammation and secondary metastasis is established.

RESULTS

Metastatic breast cancer cells contribute to the severity of arthritis in the SKG mice

In pathogen-free facilities, the SKG mice remain pro-arthritic with no macroscopic signs of joint swelling until treated zymosan A (a yeast cell wall extract) [12]. Within 30-45 days post zymosan treatment, macroscopic evidence of joint swelling in the fingers and in the fore and hind limbs is evidenced (Fig 1. a-f). SKG, SKG + zymosan (30-days post treatment) and Balb/c control mice were challenged with $1x10^6$ syngeneic breast cancer cells (4T1 being metastatic and TUBO being non-metastatic) in the mammary fat pad. Compared to the Balb/c control and the pro-arthritic SKG mice (Fig 1. a and b), the joint swelling was 5-fold higher in the 4T1 tumor-bearing SKG + zymosan mice (Fig 1. e and f) and 2-fold higher in the TUBO-bearing SKG + zymosan mice (Fig 1. c and d). The SKG + zymosan mice bearing the 4T1 tumors had a 2-fold increase in joint swelling compared to the same mice bearing the TUBO tumors (Fig 1. e and f compared to Fig 1. c and d) suggesting that the metastatic 4T1 breast cancer cells can augment the severity of arthritis. *Similar results were seen in N=8 mice per experimental group.*

Although SKG mice bearing the 4T1 or TUBO tumors did not show signs of joint swelling, histological examination of the bone sections clearly indicate severe inflammation with high degree of cellular infiltration in the joints of the 4T1 tumor-bearing SKG mice but not in the TUBO-bearing SKG mice (Fig 1. l and j). Similarly, higher severity of synovial hyperplasia and erosion of articular cartilage in the phalangeal joints of the hind limb along with severe cellular infiltration was found in the 4T1 tumor-bearing SKG + zymosan mice (Fig 1. m**)** compared to the joints of the TUBO-bearing SKG + zymosan mice (Fig 1. k)**.** Thus, it becomes clear that the metastatic 4T1 but not the non-metastatic TUBO breast cancer cells contribute to the vicious cycle of osteolytic destruction. Inflammation was not observed in zymosan-treated Balb/c mice or in saline-treated SKG mice (Fig 1. g and h**)**. *Several sections from N=8 mice per experimental group were examined with similar results. Sections of the distal hind limb joints are shown.*

Significantly higher primary breast tumor burden in pro-arthritic SKG mice as compared to the non arthritic Balb/c mice

Next we questioned if the primary tumor burden is affected by the pro-arthritic or arthritic milieu. The 4T1 and TUBO tumor burden in the SKG mice was significantly higher compared to the non arthritic Balb/c mice (Fig 1. n and o **$p<0.01$). Surprisingly, this was reversed in the SKG + zymosan mice where the primary 4T1 or TUBO tumor weight remained exactly the same as the tumor weights in the Balb/c control mice (Fig 1.

n and o). The data may indicate that the innate immune responses elicited by zymosan injection might regulate the primary tumor growth.

Significant increase in lung metastasis in the pro-arthritic and arthritic mice.

We observed a 3-fold increase in the incidence of lung metastasis in the 4T1 tumor-bearing SKG and SKG + zymosan mice compared to the 4T1 tumor-bearing Balb/c mice **(**Fig 2. a-j and Table 1. a-c**)**. One hundred percent of the SKG (8/8 mice) and SKG + zymosan (9/9 mice) mice developed lung metastasis with the 4T1 tumors compared to only 27% (3/11 mice) of the Balb/c mice (Fig 2. j and Table 1. a-c). The number and size of the lung lesions were also found to be significantly higher in the SKG versus the Balb/c mice **(**Table 1. a-c). This result is especially significant since it represents true metastasis arising from the primary mammary gland tumor. Lungs from TUBO-challenged mice show no metastatic lesions in the Balb/c or SKG mice, albeit 2/8 SKG + zymosan mice developed lung lesions (Fig 2. d-f and Table 1. d). There were no metastatic lesions in lungs of control Balb/c, SKG, and SKG-zymosan mice without tumor challenge (Fig 2. a - c, and j). A representative lung from each experimental group is shown (Fig 2. a - i).

To investigate a mechanism of the increased lung metastasis, we first examined the lung histology. It became apparently clear that all lungs that developed metastasis were packed with inflammatory cellular infiltrates characterized by prominent neutrophilic and granulocytic cells and activated macrophages **(**Fig 2. n-w). We graded the severity of lung infiltration and arbitrarily assigned levels of infiltration as ‘no’, ‘low’, ‘medium’, and ‘high’. Table 1 shows a strong correlation between the level of lung infiltration and

severity of lung metastasis in all mice. Along with the cellular infiltrates, epithelial metastatic lesions were identified in the lungs as indicated by the solid yellow arrowheads (Fig 2. s, t, u, and w). The lungs from SKG (Fig 2. n), SKG + zymosan (Fig 2. o), TUBO-bearing Balb/c (Fig 2.p), TUBO-bearing SKG (Fig 2.q), and TUBO-bearing Balb/c + zymosan (Fig 2. r), all show normal architecture and correlates with zero lung lesions (Table 1). A high degree of correlation exists between level of cellular infiltration in the lungs and lung metastasis suggesting a chemo-attractant microenvironment created in the lungs of arthritic mice for breast cancer cells to home and grow. Correlation Coefficient for lung infiltration and development of lung metastasis was calculated to be 0.99.

The next obvious question was whether the severity of lung metastasis follows the severity of arthritis. A representative lung and bone section of a 4T1 tumor-bearing SKG mouse is shown in Fig 2. k and l in which severe inflammation in the fore and hind limbs correlated with severe metastatic lung lesions. Significant correlation exists between severity of joint inflammation and the development of lung metastasis in the 4T1 tumor-bearing SKG and SKG + zymosan mice (correlation coefficient of 0.93 and 0.90) **(**Fig 2. m**).**

Increased expression of pancytokeratin positive epithelial cells in the arthritic bones coupled with increased expression of CD31 and COX-2.

Since cellular infiltration in the lungs greatly facilitated the recruitment of breast cancer cells to the site (Fig 2.), we examined if high cellular infiltration in the bones of the arthritic mice had a similar effect. We have already established that there is increased

cellular infiltration in the bones of arthritic mice challenged with the 4T1 tumors **(**Fig 1. l and m**).** We now examined the levels of pro-inflammatory factors in the bone that may create a milieu conducive for increased bone metastasis. Inflammation in the joints is usually represented by high levels of cyclooxygenase-2 (COX-2) expression which plays a critical role in fostering tumor growth. In the same context, increased platelet endothelial cell adhesion molecule (CD31) expression in the bone correlates with tumor cell homing and spreading. In comparison to the non tumor-bearing arthritic mice, the expression of COX-2 and CD31 in the bones of the 4T1 tumor-bearing arthritic mice was significantly greater (Fig 3. a – f for COX-2 and g - l for CD31). In contrast, the 4T1 tumor-bearing non-arthritic Balb/c and Balb/c + zymosan mice had minimal expression of the two proteins (Fig 3. a and c). Thus, we hypothesize that the pro-inflammatory microenvironment in the arthritic bone enhances the metastatic potential of the 4T1 tumors and that the 4T1 tumors in turn augment the severity of inflammation in the bone which creates a highly conducive microenvironment for the 4T1 tumors to home and proliferate. To directly test the presence of epithelial (tumor) cells in the inflamed bones, sections of the bone were stained with pan-cytokeratin antibody. Increased expression of pancytokeratin-positive areas was only evident in the bones of the 4T1 tumor bearing arthritic mice (Fig 3. n and p). Bones from all other experimental groups were negative (Fig 3. m, o, q, and r)**.** Brown staining represents CD31, COX-2, and pancytokeratin positivity. *Bones from n=8 mice were examined with similar staining patterns.*

Increased 4T1 bone lesions in the arthritic versus non-arthritic mice

The bones from n = 4 - 5 mice were analyzed by Faxitron imaging for osteolytic lesions. Representative images are shown in Fig 3. s - x. Osteolytic and/or sclerotic bone lesions were determined in ~50% (2/4) of SKG mice and 60% (3/5) of the SKG + zymosan mice challenged with the 4T1 metastatic tumor cells **(**Fig 3. v and w**)**. These bones show distinct radiolucencies in the distal femoral diametaphysis indicating apparent osteolytic bone lesion (as indicated by the arrows). In contrast, none of the Balb/c mice challenged with 4T1 tumors developed bone lesions (Fig 3. t) nor did any of the SKG mice challenged with TUBO cells (Fig 3. s, u, and x). The results confirm that bone lesions only occur in the pro-arthritic bones but not in non-arthritic bones (Fig 3. y).

M-CSF, IL-6, IL-17, TNF-α and VegF may be the underlying factors responsible for the increased metastasis in the arthritic mice.

To determine the possible mechanism that drives the 4T1 cells to become more metastatic in the arthritic model, we evaluated the circulating levels of pro-inflammatory cytokines and chemokines in the sera of the arthritic versus the non-arthritic mice. A custom mouse cytokine array was designed to test the sera for the presence of 10 cytokines known to be associated with AA, inflammation, and metastasis. These included macrophage colony stimulating factor (M-CSF), tumor necrosis factor-alpha (TNF-α), Interferon-gamma (IFN-γ), VegF, Interleukin-17 (IL-17), matrix metalloproteinase-2 (MMP-2), Interleukin-6 (IL-6), Insulin-like growth factor-II (IGF-II), Interleukin-1beta (IL-1β), and Interleukin-4 (IL-4) **(**Fig 4. a**)**. Compared to the 4T1 tumor-bearing Balb/c mice, significant increase in the levels of M-CSF (1.5 fold), IL-17 (1.3 fold), TNF-α, VegF and IL-6 (1.2 fold) was observed in the 4T1-bearing arthritic mice (Fig 4. e-g,). A

graphical representation of the values from the densitometric analysis is provided in Fig 4. h. In the TUBO-bearing mice, the increase was non-significant (Fig 4. b-d and h), once again implying that the increase in the cytokine levels were driven by a combination of the metastatic 4T1 tumors and AA but not by either condition alone.

DISCUSSION

A significant increase in breast cancer-associated secondary metastasis is observed in the arthritic versus the non-arthritic mice (Fig. 2 and 3). In addition, the metastatic breast cancer cells accentuate the severity of bone and lung inflammation in the arthritic mice creating a favorable microenvironment for the tumor cells to grow (Fig 1 and 2). We establish that the chronic inflammation in the bone and lung caused by AA and the subsequent increase in circulating levels of proinflammatory cytokines may be the underlying mechanism for the increased metastasis (schematically represented in Fig 5.)**.** Metastatic breast cancer cells produce factors that directly or indirectly induce the formation of osteoclasts. In turn, bone resorption by osteoclasts releases growth factors from the bone matrix that stimulate primary tumor growth, and bone destruction. This reciprocal interaction between breast-cancer cells and the bone microenvironment results in a vicious cycle that increases both bone destruction and increases tumor burden and metastasis (Fig 5.) [13]. The fact that the primary tumor burden is not increased in the SKG mice injected with zymosan (Fig 1. n and o) can be explained by the fact that zymosan, a crude yeast cell wall extract activates the arthritogenic T cells through stimulating the

innate immune response [12], which helps keep the primary tumor in check but does not reduce the incidence of metastasis.

The lungs of the arthritic mice with the 4T1 metastatic lesions express exceptionally high levels of interstitial inflammatory cellular infiltrates characterized by prominent neutrophils, mast cells, activated macrophages, and possibly eosinophils (**Fig 2. n-w**). These pro-inflammatory leukocytes alone can facilitate tumor cell extravasation and promote metastasis [14]. This is the first study that undoubtedly establishes a correlation between the pro-inflammatory cell recruitment in the lungs during AA and the homing of the circulating tumor cells in the inflamed lungs (Figure 2 and Table 1).

As in human AA, cytokines play an essential role in the development of arthritis in the SKG mice [9, 15]. Several cytokines have been implicated in the mechanism of synovial cell activation and joint destruction in AA [16]. In our study, serum analysis of cytokine proteins revealed higher expression of M-CSF, IL-17, IL-6, TNF-α, and VegF in the arthritic mice only when challenged with 4T1 metastatic breast cancer cells (Fig 4**)**. Elevated serum M-CSF predicts reduced survival in metastatic breast cancer patients. The M-CSF produced by breast cancer cells and surrounding stoma increases osteoclast formation and maturation and enhances the expression of stromal RANK ligand, both of which increase osteolytic bone degradation [17]. IL-17 has been identified as a crucial cytokine for osteoclastic bone resorption in AA patients. IL-17 acts on osteoblasts by stimulating COX-2–dependent prostaglandin E_2 (PGE_2), and osteoclast differentiation factor which differentiates osteoclast progenitors into mature osteoclasts, causing bone

resorption. PGE_2 interacts with its eicosanoid receptors to induce the damage [18]. IL-6 is an autocrine and paracrine growth factor for several cancers, including breast cancer [19] and stimulates cancer cell growth and contributes to recurrence and metastasis in breast cancer [20]. VegF is known to play a critical role in vasculogenesis, angiogenesis, and metastasis. Upregulation of these cytokines may therefore account for the enhanced breast cancer associated secondary metastasis as well as accentuating the severity of arthritis in the SKG mice. Thus, blocking these pro-inflammatory cytokines may hold promise in reducing the severity of both diseases.

Inflammation is a critical hallmark of arthritis and tumor progression [2, 21-23]. Many processes that occur during arthritis also occur during tumorigenesis. There is increased vascularity in both; and there are common cytokines and growth factors that are regulated in both. The microenvironment in the tumor and arthritis is largely orchestrated by inflammatory cells [24]. Thus, it is not unlikely that the two diseases commonly co-exist in women. Our study begins to evaluate whether these two disease states molecularly interact and feed of each other. These studies may have important clinical implications, especially in the prevention of secondary metastasis, in designing combination drug regimens, and as a diagnostic risk-assessment tool.

METHODS

Mice

SKG mice have been established from the closed breeding colony of Balb/c mice [9]. Two sets of SKG breeding pairs were purchased from CLEA International Japan and were maintained in our animal facility. All protocols were approved by the Mayo Clinic Internal Animal Care Review Committee.

Induction of Arthritis

Two month old mice were given a single intraperitoneal (ip) injection of 2mg of zymosan A in 100ul of 0.15M NaCl per mouse [12] and joint swelling was macroscopically examined starting at 14-days post zymosan A treatment. Thirty days post zymosan A, >95% of the mice develop polyarthritis in small and large joints. At this time, mice were injected with $1x10^6$ (in 100ul of phospahate buffered saline) syngeneic breast cancer cells (4T1: metastatic or TUBO: non-metastatic) in the mammary fat pad. Age-matched SKG mice without zymosan A were used as the pro-arthritic model, and Balb/c mice were used as the non-arthritic controls. Tumors were allowed to grow for 4 weeks. Zymosan A was purchased from Sigma-Aldrich, USA. A 1% solution of zymosan was made in 0.15 M sodium chloride (NaCl), placed in boiling water bath for one hour, centrifuged for 30 minutes at 4000 rpm and the residue suspended evenly in the 0.15M NaCl to the desired concentration. It is established that the glucose polymer B-1,3-D-glucans (B-glucans), the main constituents of zymosan A, are responsible for the arthritogenic effect **(12)**.

Cell Culture

The 4T1 mammary carcinoma cell line was purchased from The American Type Cell Culture Collection and the TUBO mammary carcinoma cell line was generously provided

by Dr Joseph Lustgurten, Mayo Clinic College of Medicine. 4T1 and TUBO cells were maintained in RPMI-1640 medium supplemented with 10% FBS, 1% Glutamax-1 and 1% penicillin-streptomycin. Cells were maintained at log phase at 37^0C with 5% carbon dioxide. 4T1 is a highly metastatic breast cancer cell line derived from a spontaneously arising BALB/c mammary tumor. TUBO is a cloned cell line established from a mammary carcinoma of the Her2-neu transgenic mice also on the Balb/c background. TUBO is considered to be a non metastatic cell line.

Measurement of Circulating Cytokines

The RayBio® Custom Mouse Cytokines Antibody Array kit was purchased from RayBiotech (Norcross, GA) and used according to the manufacturer's instructions. Briefly, after blocking with 1X blocking buffer (provided by the manufacturer), membranes were incubated for 1.5h with the experimental serum (10-fold diluted with 1X blocking buffer). The membranes were washed and incubated with biotin-conjugated antibodies for 1.5 h. The membranes were washed again and incubated with streptavidin-conjugated horseradish peroxidase (HRP) for 2h, washed, and developed using an enhanced chemiluminescent substrate for HRP. Chemiluminescence was detected using a EpiChemi3® Darkroom imaging system and LabWorks® densitometry software (both from UVP Bioimaging, Upland, CA). Data was corrected for background signal and normalized to positive controls using RayBio® Analysis Tool software.

Histology

Lungs and a part of the tumor were formalin fixed in 10% neutral-buffered formalin (pH 6.8-7.2) for a minimum of 24 hours. Paraffin embedded blocks were prepared by the Histology Core at The Mayo Clinic and 4-micron thick sections were cut for hematoxylin eosin (H&E) staining and for immuno-staining. For bones: The fore limb and hind limb were dissected from the mice and immersed in 10% neutral-buffered formalin (pH 6.8-7.2) overnight. For decalcification, Cal-Rite (Richard Allan Scientific, Kalamazoo, MI), a formic acid decalcification agent was used for ~72 hours followed by the conventional processing method. To determine CD31, COX-2 and Pancytokeratin expression in the bones, COX-2, CD-31, and Pancytokeratin (Santa Cruz Biotechnologies) antibodies were used at 1:50 and incubated overnight at 4◦C followed by the DAKO anti-goat secondary (1:100 dilution) for 45 minutes at RT for both COX-2 and CD-31. For Pancytokeratin staining, DAKO anti-mouse secondary was used at 1:100 for 45mins at RT. 3, 3" –Diaminobenzidine was used as the chromogen and hematoxylin was used as counterstain. Slides were examined under light microscopy and pictures taken at 200X magnification.

Faxitron Imaging: The Faxitron is a 160-kVp x-ray machine that was adapted from an x-ray imaging unit through modifications to facilitate experimental irradiation and imaging. The Faxitron model CP160 (Faxitron X-Ray Corp., Wheeling, IL, USA) is a commercially available x-ray tube machine that is designed for animal irradiation [25]**.** The analysis was conducted by a Mayo Clinic Radiologist.

Statistical analysis:

Student's t-test was used for comparing the level of significance between the experimental groups. Correlation Coefficient was determined using the JMP statistical program.

ACKNOWLEDGEMENTS

We are grateful to Dr Ronald J. Marler, our Pathologist for his guidance and immense support with interpretation of the histologic images; Drs Gendler, Lee, and Schettini, for their valuable advice during the preparation of the manuscript; Dr Spencer Chivers, our Radiologist for analyzing the Faxitron images; Leslie Dixon, and Karen Lacombe for histology; all personnel in the Mayo Clinic Animal Facility; Judy Bradley, Scott R.Dulla, Jennifer Crease, Mary Merill, and Theresa Lombari for technical support. We are extremely grateful to Sandeep Roy for preparation of the figures. This work was funded by the Concept Award BCO63396 from the Department of Defense Breast Cancer Research Program and by The Mayo Foundation.

FIGURE LEGENDS

Figure 1. **Induction of arthritis and tumor burden in SKG mice: a-f:** Images of the hind and fore limbs **a:** control Balb/c mice (no inflammation)**; b**: control SKG mice (no inflammation); **i:** control SKG + zymosan without tumor challenge (moderate inflammation); **c and d:** SKG mice + zymosan A + TUBO (low-level inflammation); **e and f**: SKG mice + zymosan A + 4T1 cells (severe swelling). **g-m:** H&E staining of

sections from the joints: **g:** Balb/c mice; **h:** SKG mice; **j:** SKG mice + TUBO cells; **k:** SKG mice + zymosan A + TUBO cells showing some erosion of articular cartilage; **l**: SKG mice + 4T1 cells showing severe inflammation in the phalangeal joints; and **m:** SKG mice + zymosan A + 4T1 cells showing severe synovial hyperplasia and erosion of articular cartilage and bone in phalangeal joints with severe inflammation; **n-o:** Tumor burden in grams (g)**n:** mice injected with 4T1 cells; **o:** mice injected with TUBO cells. Compared to the non-arthritic Balb/c mice, a significant increase in tumor burden was observed in SKG mice with 4T1 (**$p<0.01$) and TUBO cells (*$p<0.05$). *Note: All tumor cells were injected in the mammary fat pad and sacrificed 4-weeks post tumor challenge. All images taken at 200X magnification*

Figure 2. AA-related inflammation in the lungs is associated with a 3-fold increase in the number of lung metastatic lesions in the SKG mice. Representative images of lungs from **a:** Balb/c; **b:** SKG; **c:** SKG + zymosan A; **d:** Balb/c injected with TUBO cells; **e:** SKG without zymosan A + TUBO cells; **f:** SKG + zymosan A + TUBO cells (2/8 mice developed lung lesions); **g**: Balb/c + 4T1 cells (3/11 mice developed lung lesions); **h**: SKG without zymosan A + 4T1 cells (8/8 mice developed severe lung metastasis); **i:** SKG + zymosan A + 4T1 cells (9/9 mice developed severe lung metastasis). **j:** Percent mice that developed lung metastasis. **k and l:** H&E of bone section showing high inflammation and an image of lung with metastasis from the same 4T1-bearing SKG mouse**. m:** A statistical analysis for correlation of bone inflammation and lung metastasis. The correlation coefficient for the 4T1 tumor-bearing SKG and SKG + zymosan mice was determined to be 0.93 and 0.90. Correlation for TUBO-bearing mice

was not calculated. **n-w:** H&E staining of the lung sections from **n:** SKG (no infiltration); o**:** SKG + zymosan A (moderate infiltration).**p:** Balb/c + TUBO; **q:** SKG + TUBO; **r:** Balb/c + zymosan A + TUBO; **s:** SKG + zymosan A + TUBO (high infiltration)**; t:** Balb/c + 4T1 (high infiltration due to the 4T1 cells, representative of the mice that had lung metastatic lesion); **u:** SKG + 4T1 (severe infiltration); **v:** Balb/c + zymosan A + 4T1 (no infiltration); and **w:** SKG + zymosan A + 4T1 (severe infiltration). The solid filled arrow represents lung metastatic lesions, unfilled arrow represents neutrophils and unfilled circles represent macrophages. *All images taken at 200X magnification*

Figure 3. Increased expression of COX-2, CD31, and pancytokeratin in the bones of arthritic mice challenged with 4T1 cells. Bone sections from various experimental groups (indicated in the Figure) stained for COX-2 (**a-f),** CD31 (**g-l),** and pancytokeratin **(m-r)**. *Brown staining represents positive staining. All images taken at 200X magnification.* Representative Faxitron images of bones (**s-x)**. Balb/c + TUBO (**s**); Balb/c + 4T1 (**t**); SKG + TUBO (**u**); SKG + 4T1 **(v)** showing a few small radiolucencies in distal femoral diametaphysis indicating apparent osteolytic bone lesion; SKG + zymosan A + 4T1 (**w)** showing a medium size poorly defined radiolucency in the distal femoral diametaphysis possibly due to osteolytic bone lesion; and SKG+ Zymosan+ Tubo **(x).** N=4-5 mice from each group were examined using the faxitron. No lytic or sclerotic lesions were observed in any other experimental group. **y:** Percent mice that developed bone metastasis.

Figure 4. Serum analysis of cytokines revealed upregulation of several cytokines in the arthritic mice.

a. Array template of the cytokines on the membrane. **b-g.** Membrane dot blot representing circulating cytokine levels in various groups of mice (indicated in the Figure). Boxes are drawn around the cytokines that are up-regulated. **h:** A graphical representation of the up-regulated cytokines observed on the membrane blots based on densitometric analysis. Up-regulation of M-CSF, TNF-alpha, IL-17, VegF, and IL-6 is observed and highlighted in gray on the template (**a**).

Figure 5: Schematic model representing the vicious interaction between metastatic breast tumors and the inflammatory microenvironment in the bone and lung due to AA: During arthritis, neutrophils, and macrophages infiltrate the bones and lungs causing high degree of inflammation which trigger the release of pro-inflammatory cytokines (such as IL-17, IL-6, TNF-α, and VegF) in the circulation. These cytokines act directly or indirectly on the primary breast tumor cells enhancing their metastatic ability. In turn, the metastatic 4T1 breast tumor cells release more pro-survival/pro-inflammatory cytokines and invade the underlying extracellular matrix and circulate in the blood and lymphatic systems of the arthritic mice. The large amounts of inflammatory cells and pro-inflammatory cytokines in the bones and lungs attract the tumor cells to leave the circulation and enter the organs. In the bone, the tumor cells stimulate the release of IL-17 which differentiates osteoclast progenitors into mature osteoclasts, causing bone resorption. The damage to the bone matrix allows retention and growth of the tumor cells

in the site. The tumor cells also stimulate the surrounding stromal cells to release M-CSF which increases osteoclast formation and maturation which increases osteolytic bone degradation and creates a milieu suitable for tumor cells to form metastatic lesions. In the lungs, the infiltrating cells and the tumor cells release M-CSF, TNF-α, IL-6 and VegF stimulating vasculogenesis, angiogenesis and tumor growth. The final distribution of metastasis reflects the relative abundance of inflammation in the organs. Thus, we hypothesize that the increase in circulating levels of proinflammatory cytokines is the underlying factor responsible for the increased metastasis.

TABLE 1: High cellular infiltration in the lungs correlates with an increase in the number of lung metastatic lesions in the arthritic mice.

Number of lung lesions in non-arthritic Balb/c **(a)** and arthritic mice **(b and c)** challenged with 4T1 cells **(a-c)** or TUBO cells **(d).** Size and number of lung lesions are shown along with level of infiltration in the same lungs. High degree of correlation exists between cellular infiltration and metastatic lung lesions.

REFERENCES

1. de Visser, K.E. & Coussens, L.M. The inflammatory tumor microenvironment and its impact on cancer development. *Contrib Microbiol* **13**, 118-137 (2006).
2. Ziegler, J. Cancer and arthritis share underlying processes. *J Natl Cancer Inst* **90**, 802-803 (1998).
3. Franklin, J., Lunt, M., Bunn, D., Symmons, D. & Silman, A. Influence of inflammatory polyarthritis on cancer incidence and survival: results from a community-based prospective study. *Arthritis Rheum* **56**, 790-798 (2007).
4. Mellemkjaer, L. *et al.* [Rheumatoid arthritis and risk of cancer]. *Ugeskr Laeger* **160**, 3069-3073 (1998).
5. Askling, J. *et al.* Haematopoietic malignancies in rheumatoid arthritis: lymphoma risk and characteristics after exposure to tumour necrosis factor antagonists. *Ann Rheum Dis* **64**, 1414-1420 (2005).

6. Askling, J. *et al.* Risks of solid cancers in patients with rheumatoid arthritis and after treatment with tumour necrosis factor antagonists. *Ann Rheum Dis* **64**, 1421-1426 (2005).
7. Minn, A.J. *et al.* Genes that mediate breast cancer metastasis to lung. *Nature* **436**, 518-524 (2005).
8. Mundy, G.R. Metastasis to bone: causes, consequences and therapeutic opportunities. *Nat Rev Cancer* **2**, 584-593 (2002).
9. Sakaguchi, N. *et al.* Altered thymic T-cell selection due to a mutation of the ZAP-70 gene causes autoimmune arthritis in mice. *Nature* **426**, 454-460 (2003).
10. Hata, H. *et al.* Distinct contribution of IL-6, TNF-alpha, IL-1, and IL-10 to T cell-mediated spontaneous autoimmune arthritis in mice. *J Clin Invest* **114**, 582-588 (2004).
11. Firestein, G.S. Evolving concepts of rheumatoid arthritis. *Nature* **423**, 356-361 (2003).
12. Yoshitomi, H. *et al.* A role for fungal {beta}-glucans and their receptor Dectin-1 in the induction of autoimmune arthritis in genetically susceptible mice. *J Exp Med* **201**, 949-960 (2005).
13. David , G.R. Mechanisms of bone metastasis. *N Eng J Med* **350:1655-64** (2004).
14. Slattery, M.J., Liang, S. & Dong, C. Distinct role of hydrodynamic shear in leukocyte-facilitated tumor cell extravasation. *Am J Physiol Cell Physiol* **288**, C831-839 (2005).
15. Sakaguchi, S. & Sakaguchi, N. Regulatory T cells in immunologic self-tolerance and autoimmune disease. *Int Rev Immunol* **24**, 211-226 (2005).
16. Arend, W.P. & Dayer, J.M. Inhibition of the production and effects of interleukin-1 and tumor necrosis factor alpha in rheumatoid arthritis. *Arthritis Rheum* **38**, 151-160 (1995).
17. K. Leitzel, E.S., Walsh.R, Abraham.J, Modur.V, Braendle.E, Evans.D.B, Ali.S.M, Demers.L and A. Lipton Elevated serum M-CSF level predicts reduced survival in metastatic breast cancer patients. *Journal of clinical oncology* **25** (2007).
18. Kotake, S. *et al.* IL-17 in synovial fluids from patients with rheumatoid arthritis is a potent stimulator of osteoclastogenesis. *J Clin Invest* **103**, 1345-1352 (1999).
19. Ben-Baruch, A. Inflammation-associated immune suppression in cancer: the roles played by cytokines, chemokines and additional mediators. *Semin Cancer Biol* **16**, 38-52 (2006).
20. Leek, R.D. & Harris, A.L. Tumor-associated macrophages in breast cancer. *J Mammary Gland Biol Neoplasia* **7**, 177-189 (2002).
21. Coussens, L.M. & Werb, Z. Inflammation and cancer. *Nature* **420**, 860-867 (2002).
22. Philip, M., Rowley, D.A. & Schreiber, H. Inflammation as a tumor promoter in cancer induction. *Semin Cancer Biol* **14**, 433-439 (2004).
23. Clevers, H. At the crossroads of inflammation and cancer. *Cell* **118**, 671-674 (2004).
24. Balkwill, F., Charles, K.A. & Mantovani, A. Smoldering and polarized inflammation in the initiation and promotion of malignant disease. *Cancer Cell* **7**, 211-217 (2005).

25. Woo, M.a.N., RA Commissioning and evaluation of a new commercial small rodent x-ray irradiator. *Biomedical imaging and intervention journal* **2**, 1-5 (2006).

Figure 1

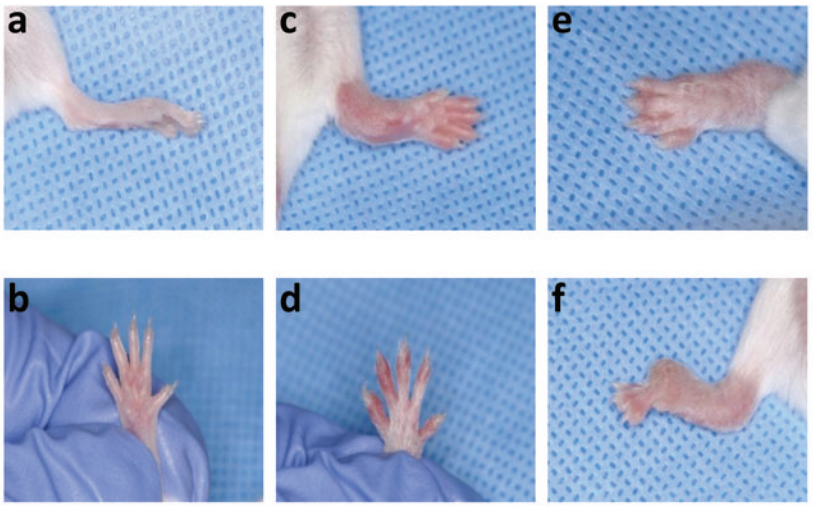
a
c
e
b
d
f

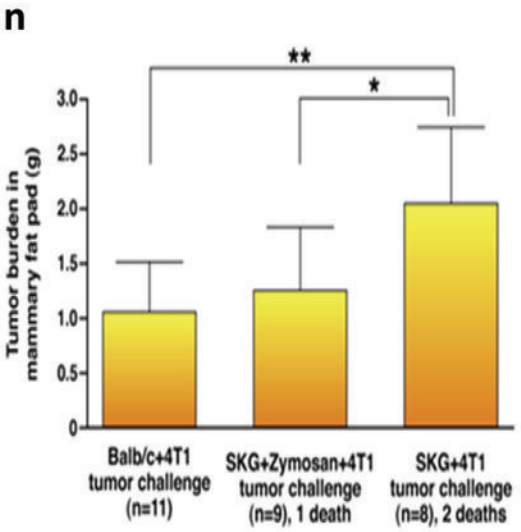
n
**
*
Tumor burden in mammary fat pad (g)
3.0
2.5
2.0
1.5
1.0
0.5
0
Balb/c+4T1 tumor challenge (n=11)
SKG+Zymosan+4T1 tumor challenge (n=9), 1 death
SKG+4T1 tumor challenge (n=8), 2 deaths

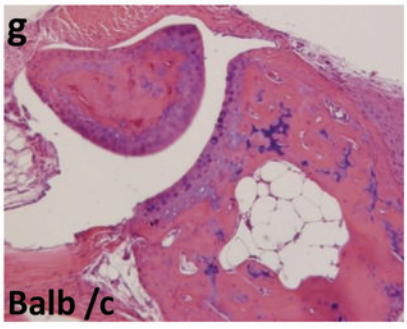
g
Balb /c

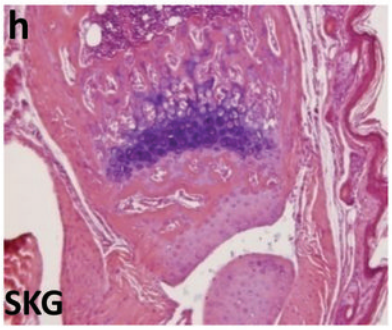
h
SKG

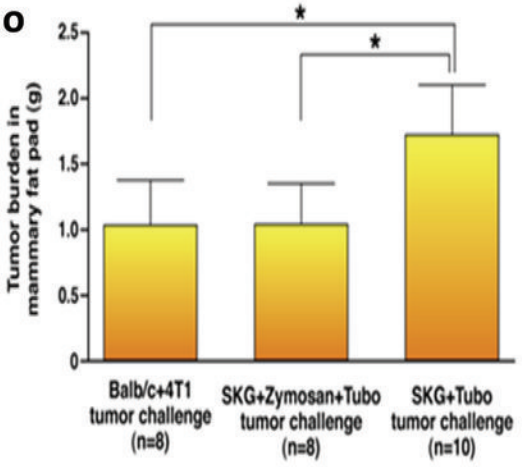
o
*
*
Tumor burden in mammary fat pad (g)
2.5
2.0
1.5
1.0
0.5
0
Balb/c+4T1 tumor challenge (n=8)
SKG+Zymosan+Tubo tumor challenge (n=8)
SKG+Tubo tumor challenge (n=10)

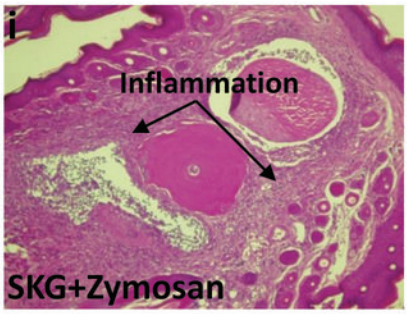
i
Inflammation
SKG+Zymosan

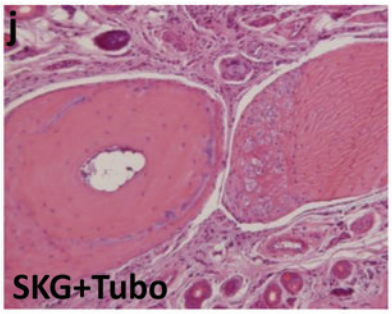
j
SKG+Tubo

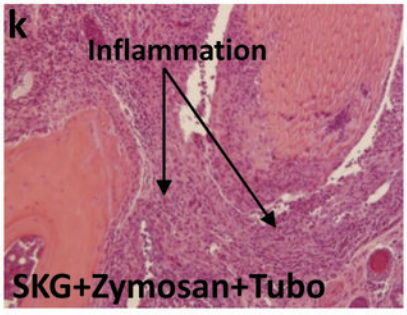
k
Inflammation
SKG+Zymosan+Tubo

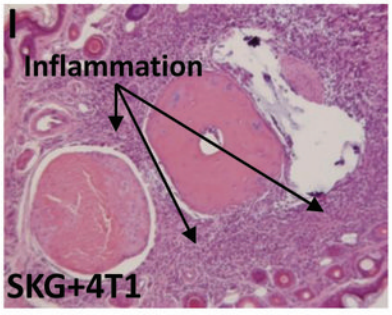
l
Inflammation
SKG+4T1

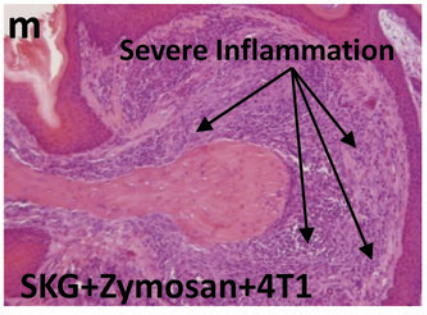
m
Severe Inflammation
SKG+Zymosan+4T1

Figure 2

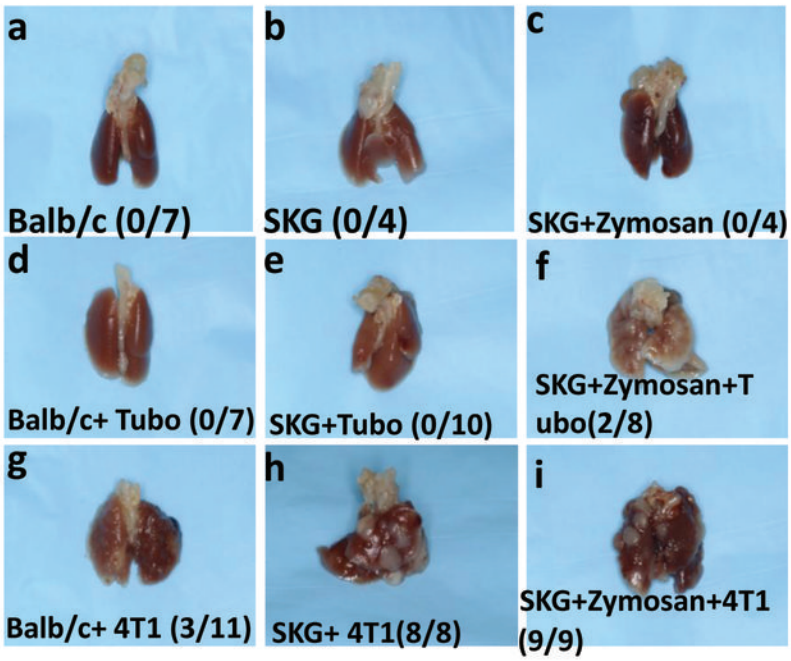
a
Balb/c (0/7)
b
SKG (0/4)
c
SKG+Zymosan (0/4)
d
Balb/c+ Tubo (0/7)
e
SKG+Tubo (0/10)
f
SKG+Zymosan+Tubo(2/8)
g
Balb/c+ 4T1 (3/11)
h
SKG+ 4T1(8/8)
i
SKG+Zymosan+4T1 (9/9)

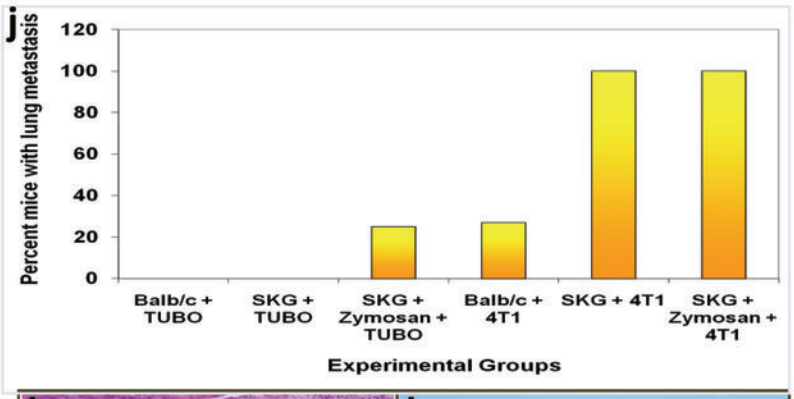
j
Percent mice with lung metastasis
120
100
80
60
40
20
0
Balb/c + TUBO
SKG + TUBO
SKG + Zymosan + TUBO
Balb/c + 4T1
SKG + 4T1
SKG + Zymosan + 4T1
Experimental Groups

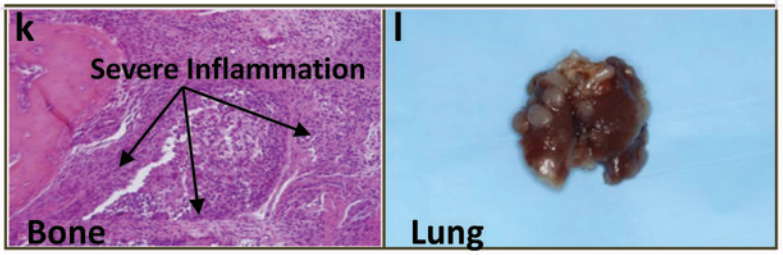
k
Severe Inflammation
Bone
l
Lung

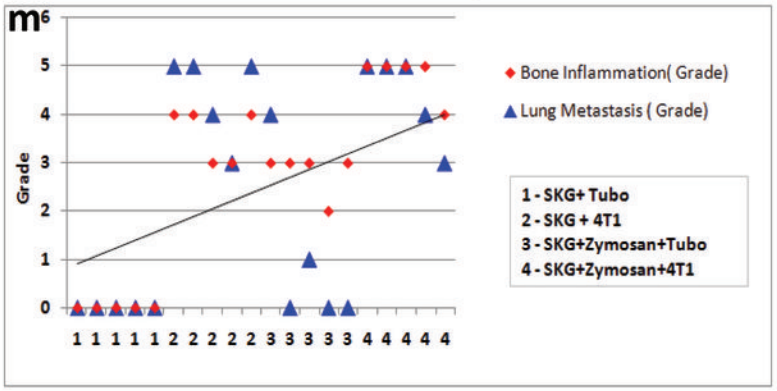
m
6
5
4
3
2
1
0
Grade
1 1 1 1 1 2 2 2 2 2 3 3 3 3 3 4 4 4 4 4
Bone Inflammation(Grade)
Lung Metastasis (Grade)
1 - SKG+ Tubo
2 - SKG + 4T1
3 - SKG+Zymosan+Tubo
4 - SKG+Zymosan+4T1

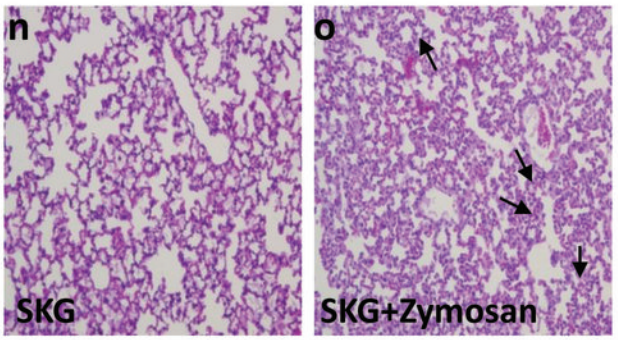
n
SKG
o
SKG+Zymosan

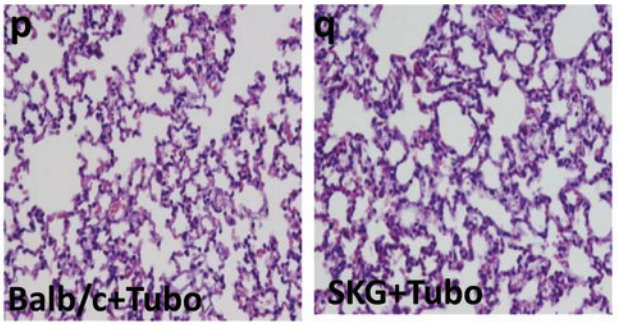
p
Balb/c+Tubo
q
SKG+Tubo

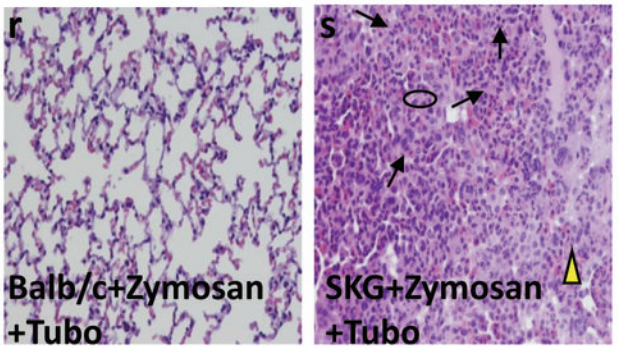
r
Balb/c+Zymosan +Tubo
s
SKG+Zymosan +Tubo

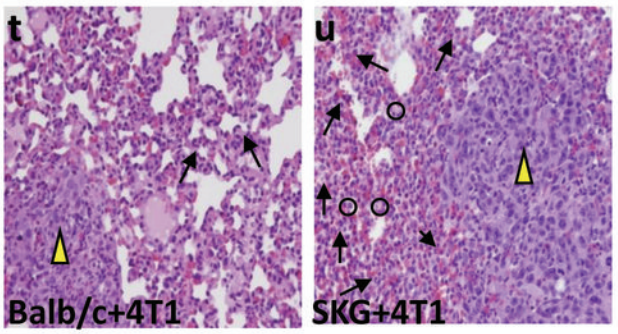
t
Balb/c+4T1
u
SKG+4T1

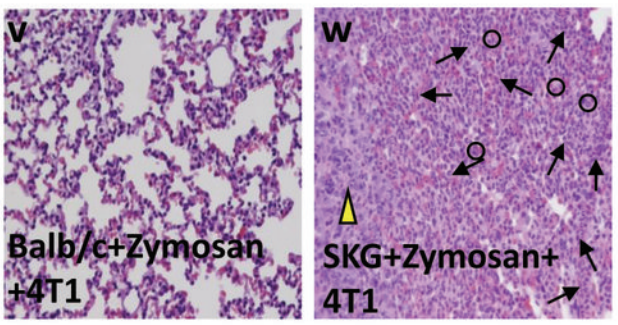
v
Balb/c+Zymosan +4T1
w
SKG+Zymosan+ 4T1

Figure 3

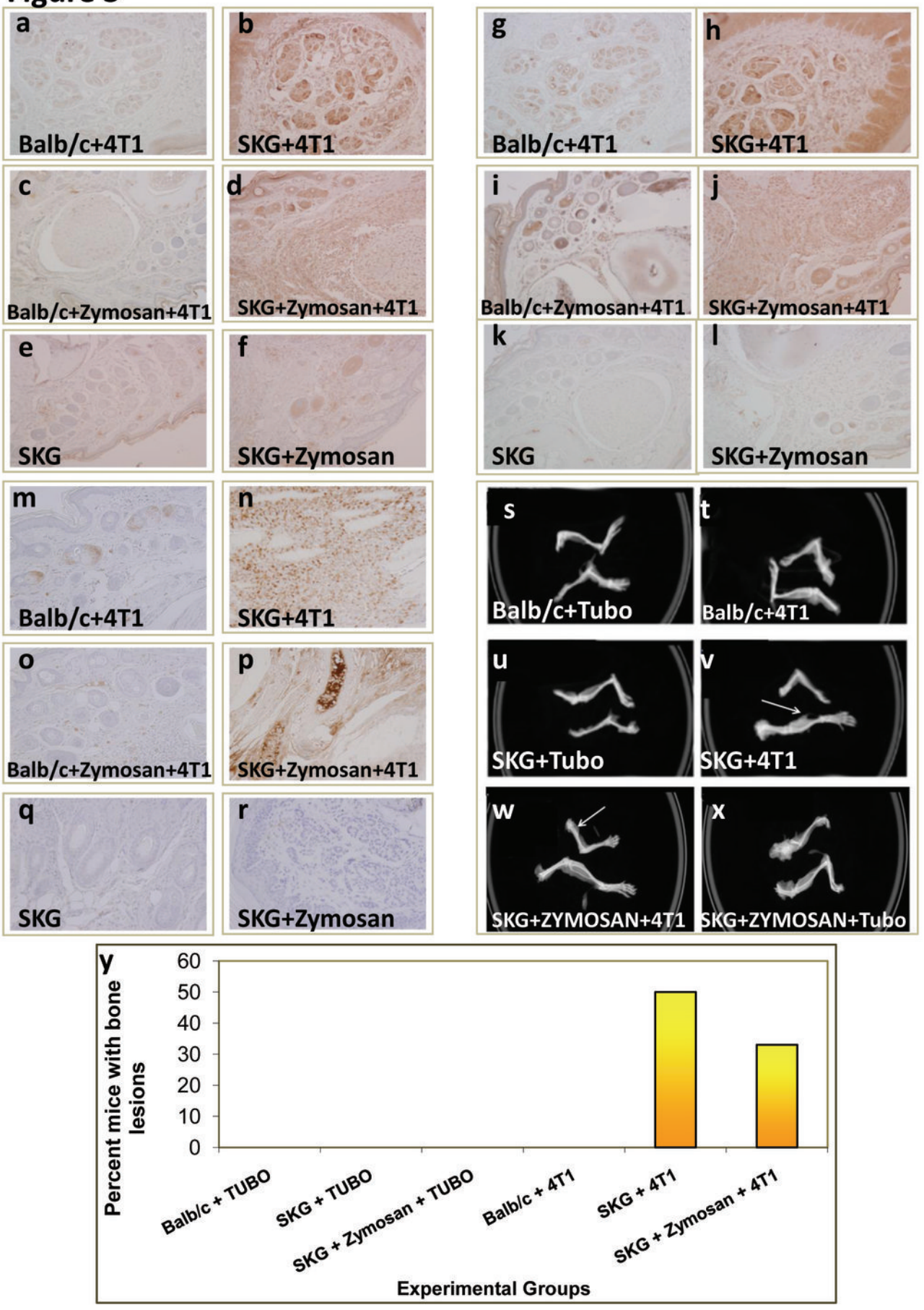
a
Balb/c+4T1
b
SKG+4T1
g
Balb/c+4T1
h
SKG+4T1
c
Balb/c+Zymosan+4T1
d
SKG+Zymosan+4T1
i
Balb/c+Zymosan+4T1
j
SKG+Zymosan+4T1
e
SKG
f
SKG+Zymosan
k
SKG
l
SKG+Zymosan
m
Balb/c+4T1
n
SKG+4T1
s
Balb/c+Tubo
t
Balb/c+4T1
o
Balb/c+Zymosan+4T1
p
SKG+Zymosan+4T1
u
SKG+Tubo
v
SKG+4T1
q
SKG
r
SKG+Zymosan
w
SKG+ZYMOSAN+4T1
x
SKG+ZYMOSAN+Tubo
y
Percent mice with bone lesions
60
50
40
30
20
10
0
Balb/c + TUBO
SKG + TUBO
SKG + Zymosan + TUBO
Balb/c + 4T1
SKG + 4T1
SKG + Zymosan + 4T1
Experimental Groups

Figure 4

a RayBio®Cytokine Antibody Arrays-Custom Array

	A	B	C	D	E	F	G	H
1	Pos	Pos	Neg	Neg	IL-17	IL-6	IL-1beta	IL-4
2	Pos	Pos	Neg	Neg	IL-17	IL-6	IL-1beta	IL-4
3	M-CSF	TNF-alpha	IFN-gamma	VEGF	MMP-2	IGF-II	Blank	Pos
4	M-CSF	TNF-alpha	IFN-gamma	VEGF	MMP-2	IGF-II	Blank	Pos

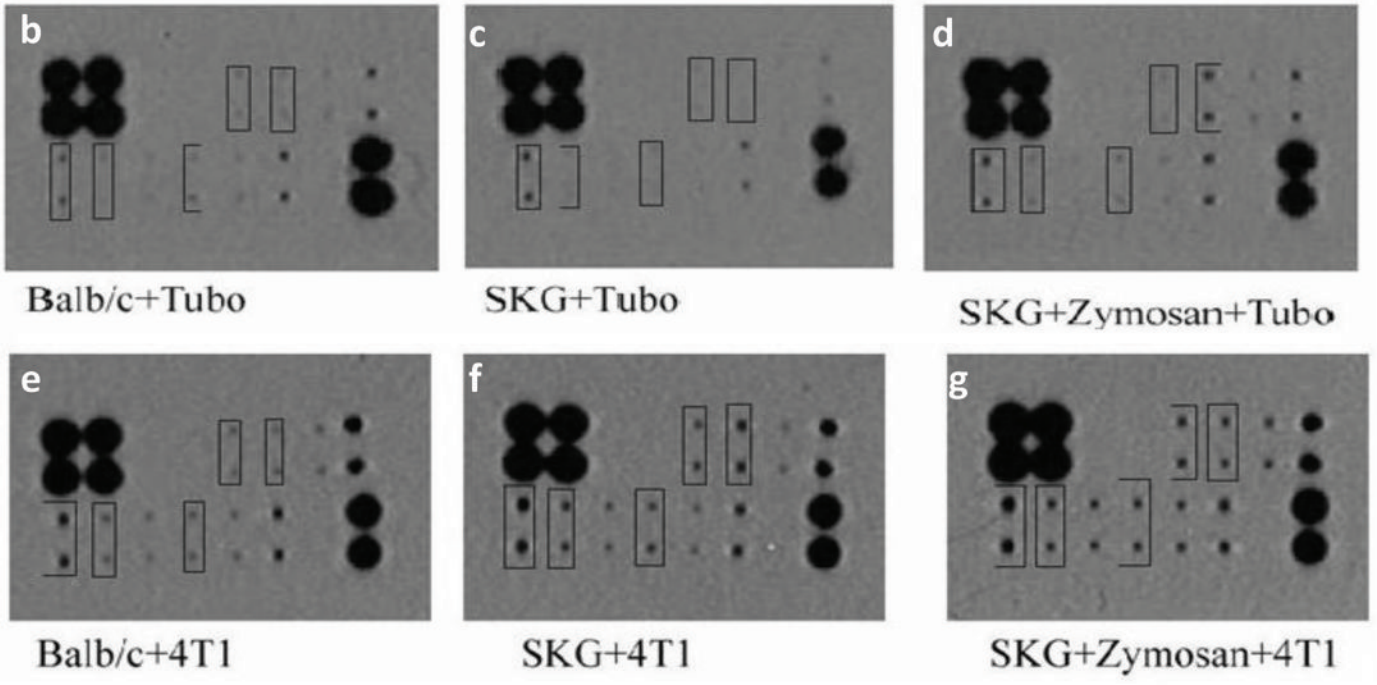

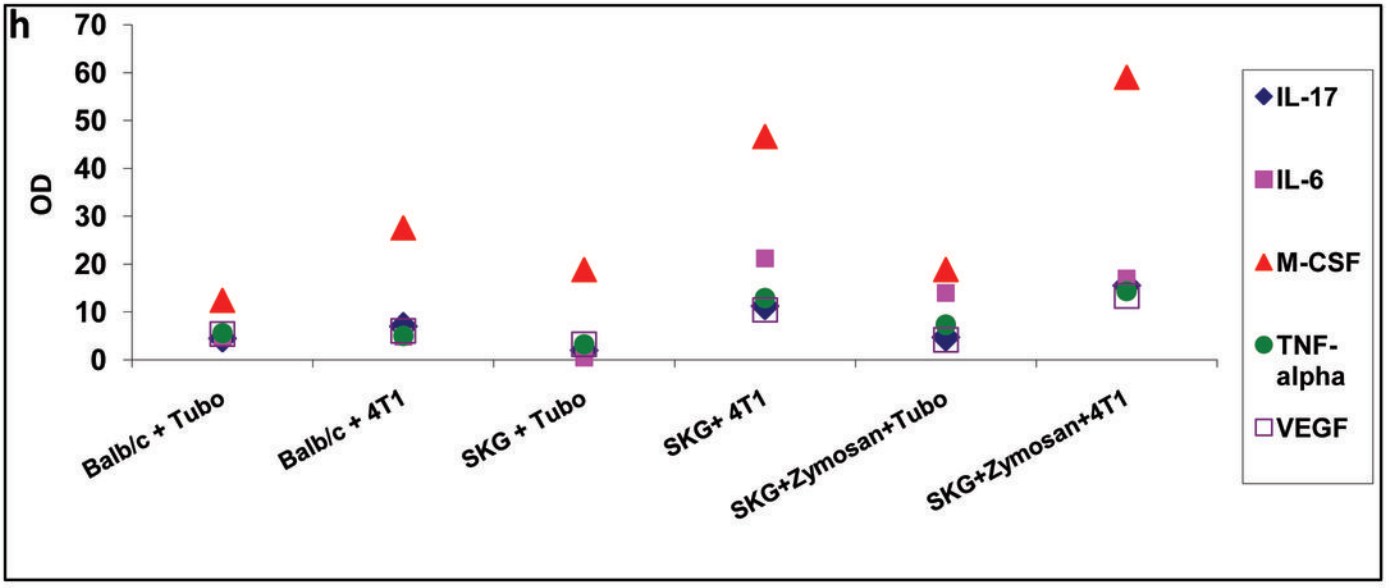

Figure 5

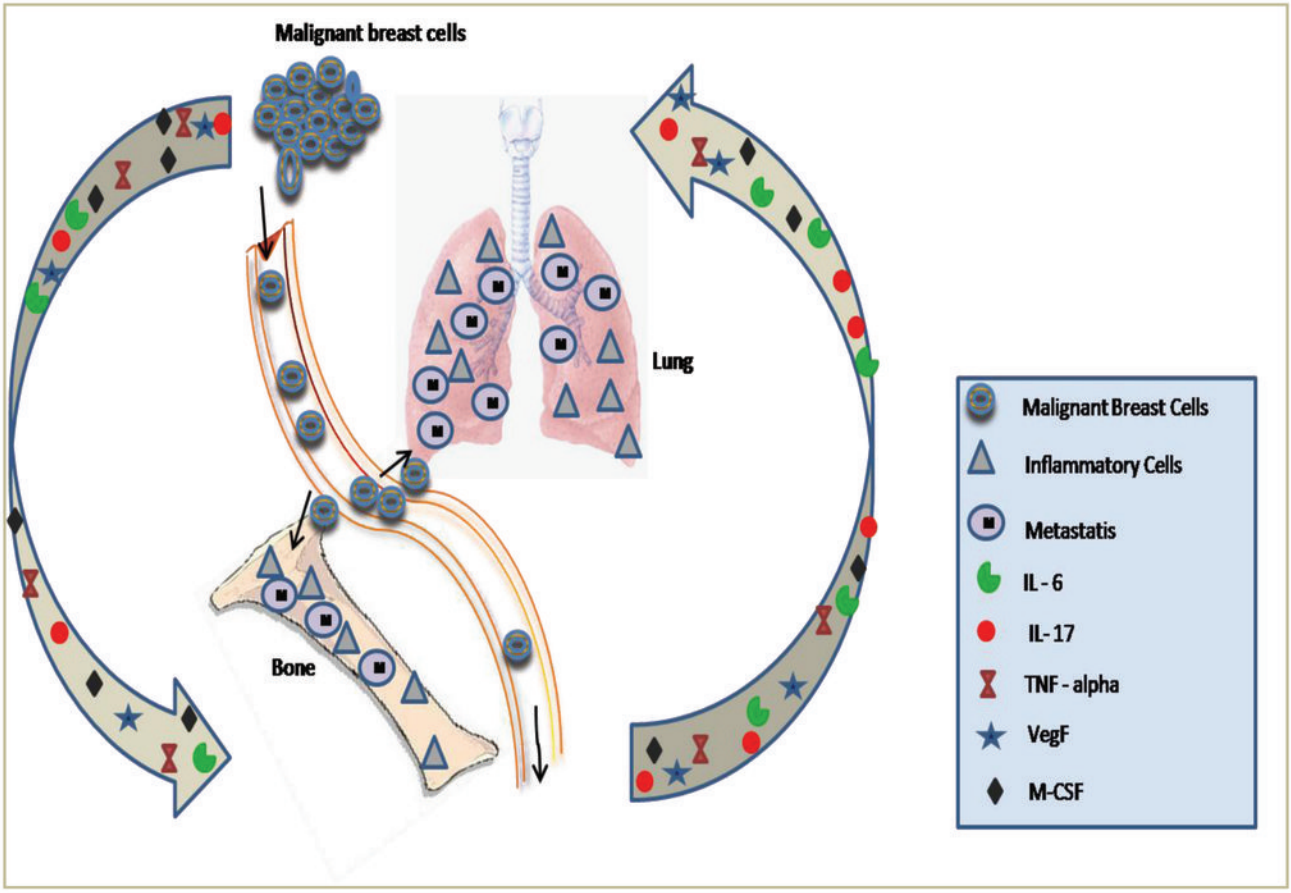
Malignant breast cells
Lung
Bone
Malignant Breast Cells
Inflammatory Cells
Metastatis
IL - 6
IL - 17
TNF - alpha
VegF
M-CSF

Table 1

Group	Mice #	Infiltrating cells in the lungs (High/Medium/Low)	Size of Lung Lesions			# Lung Lesions
			Large	Medium	Small	Total
(a) Balb/c+4T1(3/11)	1	No	0	0	0	0
	2	No	0	0	0	0
	3	No	0	0	0	0
	4	No	0	0	0	0
	5	No	0	0	0	0
	6	Low	8	0	9	17
	7	No	1	0	0	1
	8	No	0	0	0	0
	9	No	0	0	0	0
	10	No	0	0	0	0
	11	No	0	0	2	2
(b) SKG+4T1(8/8)	1	High	16	0	9	25
	2	High	10	0	11	21
	3	High	0	22	0	22
	4	High	15	0	5	20
	5	High	2	0	10	12
	6	High	0	0	13	13
	7	Medium	0	0	9	9
	8	High	0	0	14	14
(c) SKG+zymosan+4T1(9/9)	1	Medium	0	3	0	3
	2	Medium	2	0	4	6
	3	High	10	0	9	19
	4	Low	0	0	0	3
	5	Medium	0	0	0	5
	6	Medium	0	0	5	5
	7	Medium	0	1	7	8
	8	High	9	0	9	18
	9	High	0	10	6	16
(d) Balb/c+Tubo(0/7)	No lesions	No				
SKG+Tubo(0/10)	No lesions	No				
SKG+zymosan+Tubo(2/8)	1	Low	0	0	0	0
	2	Low	0	0	0	0
	3	Low	0	0	0	0
	4	Low	0	0	0	0
	5	Low	0	0	0	0
	6	Low	0	0	0	0
	7	Medium	0	10	0	10
	8	Medium	0	4	0	4